Results in Optics 2 (2021) 100039

Contents lists available at ScienceDirect

Results in Optics

journal homepage: www.elsevier.com/locate/rio

Analysis and performance of edge filtering interrogation scheme for FBG sensor using SMS fiber and OTDR

Koustav Dey [a], Sourabh Roy [a,*], Putha Kishore [a], Madhuvarasu Sai Shankar [a], Ramesh Kumar Buddu [b], Rajeev Ranjan [c,*]

[a] National Institute of Technology, Warangal, Telangana 506004, India
[b] Institute for Plasma Research, Gujarat, India
[c] CHT @Erzelli, Nanoscopy, Istituto Italiano Di Tecnologia, Genova, Genova 16152, Italy

ARTICLE INFO

Keywords:
Interrogation technique
Edge filter
Fiber Bragg gratings (FBGs)
Single-multi-Singlemode (SMS) fiber
Optical time domain reflectometry
Strain measurement
Temperature measurement

ABSTRACT

An interrogation technique for fiber Bragg grating (FBG) sensor is devised with customized in-line edge filtering single-multi-single mode fiber (SMS) component and optical time-domain reflectometer (OTDR). The performance of the proposed SMS-OTDR interrogation is established by temperature and strain sensing analysis of a standard FBG. The temperature and strain sensitivity values which are verified by theoretical analysis are estimated as 1.01×10^{-2} dB/℃ and 3.9×10^{-4} dB/με respectively. Furthermore, we have optimized and achieved controlled etching on FBG and tested it for hiking the sensitivity. Using the etched FBG, an enhanced temperature and strain sensitivity of 6.7×10^{-2} dB/℃ and 3.2×10^{-3} dB/με covering the range of 20–200 °C and 100–2015 με respectively are also recorded and analysed by this integration method. Eventually, the efficiency and cost-effectiveness of the proposed method are compared with various reported techniques and presented here.

1. Introduction:

Fiber Bragg grating (FBG) based fiber optic sensor has proven its efficient applications in various fields like structural health monitoring, oceanology, magnet field, biomedical, military, avionics and so on (Loyez et al., 2015; Kinet et al., 2014; Guerra et al., 2019; Berruti et al., 2016; Leal-Junior et al., 2018; Vaddadi et al., 2020; Chaudhuri and Pradhan, 2018; Ma and Chen, 2019). FBG sensor is having potential inherent features like lightweight, high sensitivity, immune to electromagnetic interference, remote sensing, and multiplexing. Moreover, it yields precise, accurate and stable estimations as it explores the characteristic wavelength for measuring the sensing parameters. However, any parameters being sensed by the FBG are spectrally encoded in terms of wavelength shifts. So, an interrogation technique is needed to decode the spectral changes. Several interrogations and multiplexing techniques have been reported in this purpose (Frazao et al., 2006; Li et al., 2011; Diaz et al., 2018; Po et al., 2003). Most of the reported techniques of FBG sensor analysis employed an optical spectrum analyser (OSA) to extract either wavelength or bandwidth information(s). The measurements by OSA are very accurate and precise but it is challenging to use in the practical field of application due to bulky size and high cost. So, alternative interrogation techniques of FBG sensors are always useful for the successful implementation of this sensor. The fast and cost-effective interrogation technique can be developed using an edge-filtering technique which works on frequency-to-amplitude conversion principle. Well reported edge filtering interrogation techniques using Fabry-Perot (FP) filter (Li et al., 2011; Nguyen et al., 2009; Uchimura et al., 2014; Xiong et al., 2014; Pan et al., 2015; Liu et al., 2014; Markowski et al., 2017) and long-period gratings (LPGs) (Ranjan et al., 2017; Ascorbe et al., 2018; Esposito et al., 2019; Patrick et al., 1996) established their efficiency though there are some limitations in every method. FP based filter techniques provide some advantages but limited due to the using of costly equipment. In-line fiber optic FBG-LPG sensors became popular nowadays but the broad spectral response of the LPG imposes limitations on multiplexing. It is also limited due to its complicated demodulation technology. Employing PM fiber (Uchimura et al., 2014; Ranjan et al., 2017; Esposito et al., 2019) is expensive for common fiber sensing system and also interrogating two modes in PM fiber require special set up at the receiver which increases the system cost. O. Frazao et al., reported an FBG based interrogation where high-birefringence fiber loop mirror acts as an edge filter. Although the sys-

* Corresponding authors.
E-mail addresses: koustavdey@student.nitw.ac.in (K. Dey), sroy@nitw.ac.in (S. Roy), msainitw@gmail.com (M.S. Shankar), buddu@ipr.res.in (B. Ramesh), rajeev.ranjan@iit.it (R. Ranjan).

https://doi.org/10.1016/j.rio.2020.100039
Received 30 September 2020; Revised 1 December 2020; Accepted 13 December 2020

tem is capable to integrate an array of FBG to discriminate strain and temperature simultaneously with higher resolution but limited due to OSA (Frazao et al., 2006). Hence an alternative to OSA, few interrogation techniques are reported using photodetector and optical power meter (Diaz et al., 2018; Wu et al., 2009; Barrera and Sales, 2013). Camilo A.R. Diaz et al., proposed the interrogation technique using an optical power meter, amplified spontaneous emission (ASE) broadband light source, Raman fiber laser and a Peltier with its temperature controller (TEC) for temperature and strain FBG sensor (Xiong et al., 2014). They have demonstrated a high contrast in-line FPI microcavity for building an interrogation system with high stability and repeatability. But the system is composed by some expensive components and the spatial resolution of the proposed interrogation system is limited by half free spectrum range (FSR) of the micro-cavity (5 nm.

In comparison to FP filter and LPG, a cost-effective edge filtering in-line fiber optic component can be utilised as an optimized combination of single-multi-single mode fiber (SMS) which is obtained by splicing a sandwich like the structure of a multimode fiber (MMF) with two single-mode fibers (SMFs). Wu et al. (2009) integrated an FBG using an SMS as an edge filter in a ratiometric measurement to measure strain and temperature with high resolution in strain and temperature. But the main challenge of this method is that the SMS and the FBG should have to maintain at the same temperature sensitivity i.e., 10 pm/℃ for efficient edge filtering. Furthermore, SMS is very much sensitive to the temperature and strain compared to the FBG (Wang et al., 2013; Tian et al., 2017). Hence, it is too difficult to achieve a similar shift of both the SMS and the FBG as both of the components are equally exposed.

A major simplification in the interrogation scheme can be achieved by using conventional optical time-domain reflectometer (OTDR) as it is easy to operate, handy, low energy consumption and compatible with portable power supply (Stopiński et al., 2019). The most distinct superiority of an OTDR over other optical testing techniques is that an OTDR only needs access to one end of fiber link (Tian et al., 2017). If an FBG with reflection peak coinciding with that of the bandwidth of the light source of the OTDR, it can measure the reflected signal even with very small peak reflectivity (Wang et al., 2013). Furthermore, OTDR is performed with a low coherent light source, which is affected little by polarization noise/fading noise, thereby accurately compensating for fiber losses. Though some methods have been reported (Yu-Lung, 2007; Valente et al., 2002; Bravo et al., 2012, 2011; Bolognini et al., 2007; Zhang et al., 2003; Hatta et al., 2013a, 2013b; Wang et al., 2015) using the amplitude detection of the optical signals reflected by FBG by means of OTDR it can be explored in further extent. Recently, Y. Song et al. reported an alternative of the OTDR, where distributed sensing as well as the real-time fiber fault detection is possible simultaneously with higher tunable range (Song et al., 2019). The large wavelength tuning range enables an excellent multiplexing ability, which is very important in modern large-scale sensing system. However, this technique is limited by the sampling rate of the data acquisition (DAQ) card and requires a special set-up which increases the cost of the system.

Keeping all these aspects in mind, an alternative method of interrogation of FBG sensor is proposed here using an optimized SMS edge filter with higher filtering range (~8 nm) and OTDR. Also, the SMS is used here exclusively for edge filtering and kept out of the exposed area to overcome the challenges reported in Ref (Wu et al., 2009). To our best knowledge, such SMS, OTDR interrogation technique using FBG sensor is not reported yet. As SMS is customized in the laboratory with fiber splicing machine and OTDR is readily available equipment, the whole set up will become cost-effective. The performance of proposed interrogation is tested by through strain-temperature analysis of FBG sensor. Using the proposed interrogation technique, the performance of FBG sensor is analysed thoroughly. It exhibits sensitivities of 10.1×10^{-3} dB/℃ and 3.9×10^{-4} dB/με for temperature and strain, respectively which also have been verified theoretically. Further, an etched FBG has tested here to obtain enhancement in the sensitivity. We recorded the remarkable enhancement in sensitivity of 6.7×10^{-2} dB/℃ and 3.2×10^{-3} dB/με covering the range of 20–200 ℃ and 100–2015 με for temperature and strain, respectively.

2. Experimental set-up and principle of measurement

2.1. Experimental set-up

The schematic of the experimental setup (Fig. 1) of the designed and developed sensor consists of an optical time-domain reflectometer (OTDR), an FBG (8.2/125 μm) of central wavelength 1533 nm and an SMS. The OTDR (JDSU MTS 8000 series,) is used to emit the light and detect the event induced by the temperature and strain change on the FBG in terms of optical power variation. A pulsed broadband light with central wavelength 1550 + /-20 nm from OTDR output is coupled to the sensing fiber integrated with FBG in the end part of the fiber.

When the light arrives at the FBG position, the light will be reflected by FBG. The reflected light is first filtered by the SMS, then received by OTDR.

For temperature sensing, the FBG is placed inside an oven which is connected with a dimmer stat for controlling the temperature with respect to time. A calibrator thermometer (CL3515R, OMEGA,) is employed to measure the temperature inside the oven. To investigate the influence of strain on the sensor a standard procedure is followed where the FBG is glued on the simple beam cantilever with the dimension of (15x2.5x0.1) cm made of stainless steel. The strain is applied and it is monitored using electric strain gauges. Thus, by measuring the intensity of the reflection peaks associated with the FBG sensor with OTDR it becomes possible to determine its strain and temperature sensitivity.

2.2. Principle of measurement

A fast and cost-effective interrogation is usually referred to as edge filtering technique. It works on frequency-to-amplitude conversion based on the convolution between both the FBG and the edge filter i.e., SMS spectra and the same is presented here. Due to the edge filtering property, (Hatta et al., 2013) the SMS fiber has several transmission loss dips with steep rising and falling edges, which made it ideal to be used in interrogation technique. An FBG of central wavelength 1533 nm and an SMS spectrum ranging from 1531 nm to 1539 nm are employed for this purpose. When the light travels through the SMS, the output power would linearly change with the wavelength of the input light, which is a typical linear filter. A higher slope of around 8 nm of the SMS is incorporated in the sensing system to achieve better resolution for the proposed sensor.

Due to the function of SMS, the power of the light detected by OTDR will vary linearly with the wavelength of the reflected light. The transfer function of the SMS in the linear region can be expressed as (Wang et al., 2015):

$$P_{Out} = (E_1\lambda_i + E_2)P_{In} \tag{1}$$

where λ_i is the wavelength of the light injected to the SMS; P_{Out} is the output power of the SMS; E_1 and E_2 represent the slope windows of the SMS spectrum corresponding to the falling and rising slope regions and P_{In} is the power of the input light.

The change of the central wavelength of the FBG due to the external perturbation such as temperature or strain (Hill and Meltz, 1997) can be expressed as:

$$\Delta\lambda = (1 - p_e)\varepsilon + (\alpha_\Lambda + \alpha_n)\Delta T \tag{2}$$

where $\Delta\lambda$ is the change of the wavelength due to the external perturbation; ε and ΔT are the strain and temperature change, respectively; p_e is the effective strain-optic constant; α_Λ and α_n are the thermal expansion and thermo-optic coefficient of the fiber respectively.

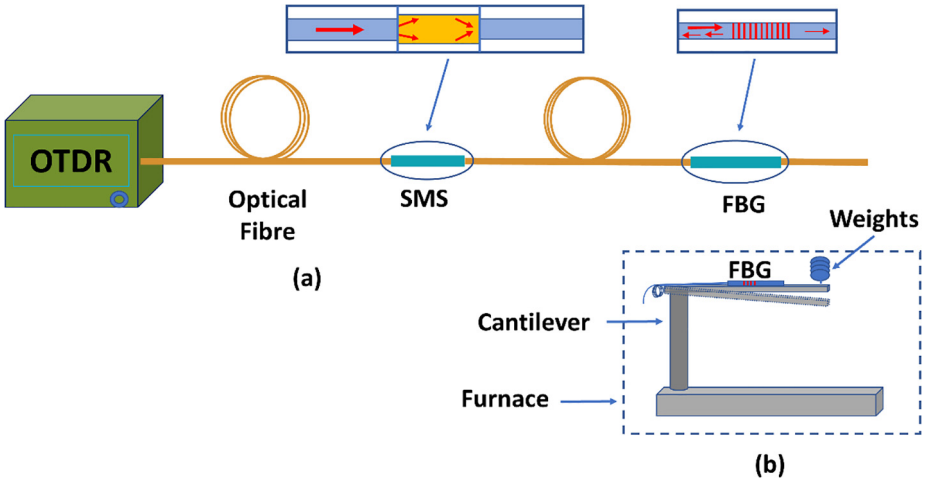

Fig. 1. (a) Schematic configuration of the experimental setup and (b) Detailed schematic of the experimental setup for strain and temperature characterization.

By substituting the Eq. (2) into Eq. (1), the wavelength shift of the FBG can be converted to the power change by SMS:

$$\Delta P = P_{In} * [E_1(1 - p_e)\varepsilon + E_1(\alpha_\Lambda + \alpha_n)\Delta T] \quad (3)$$

From the above equation, it is clear that the power of the reflected light detected by the OTDR will vary linearly with the change of strain and temperature applied on the FBG.

Therefore, the change of the wavelength of the FBG caused by the temperature or strain can be interrogated by just detecting the wavelength shift instead of demodulating the wavelength shift. As the rising slope edges have not been considered in our edge filtering technique due to the redshift property of the FBG, hence E_2 was discarded.

In order to understand the effect of the slope region of the linear region of the SMS on the sensitivity of the sensor, we further analyse the Eq. (3).

From Eq. (3) it can be seen that the variation of the power is directly proportional to E_1, which depends on the slope region of the linear filter i.e., SMS.

Let P_e is the power of the effective spectrum of the input light source and E_e is the slope of the power within the effective spectrum, then Eq. (1) can be described as

$$P_{Out} = (E_1\lambda_i)P_{In} = (E_1\lambda_i)(1 + E_e)P_e \quad (4)$$

As shown in Eq. (4), still the power of the output light linearly increases with wavelength. Thus if we assume that the effective spectrum of the input light is flat, then as the slope region increase from E_1 to $E_1 \times (1 + E_e)P_e$, the sensitivity of the sensing system could be improved to a higher value. Hence higher slope region of the edge filter leads to the higher sensitivity.

Fig. 2 shows the graphical representation of the proposed interrogation method extracted from OSA. Here we have investigated the variation of the optical power reflected from the FBG peak, which lies in one of the ripple-free steep falling edge regions of the SMS ranging from 1531 to 1539 nm as shown in Fig. 2. The dotted peaks following the linear slope edge of the SMS are the spectral variations of the FBG peak due to the external perturbation i.e., temperature and strain. The interrogation range (highlighted region) is limited by the length of the MMF.

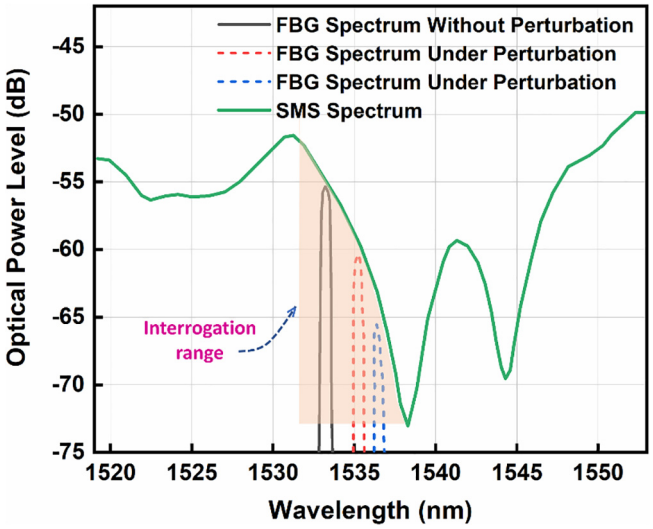

Fig. 2. Interrogation of FBG and the SMS. The FBG peak follows the linear falling edge region of the SMS. Interrogation range is shown by the shaded region.

3. Fabrication details

3.1. Fabrication of edge filter SMS

SMS fiber structure has been employed as an edge filter in our proposed interrogation technique. SMS fiber composed of two sections of single-mode and one section multi-mode fiber (MMF) which are assumed to be aligned along the same axis. The underlying principle in such hetero-core spliced scheme is multi-mode interference (MMI). The light injected into the MMF from a single-mode fiber will excite the multimode propagating through the MMF. This multimode will couple to the output SMF. As a result, the wavelength-dependent transmission spectrum can be observed due to the interference (Song et al., 2019; Kumar et al., 2003). By proper selection of the MMF length, the SMS structure can have a spectral response with falling and rising edges for a desire wavelength range. Thus, one of the steep edges of the bandpass response can be implemented in the edge filtering technique.

For fabrication of SMS fiber, first, the jacket and the coating of the multi-mode and single-mode optical fiber are peeled using a fiber stripper. After that, the optical fiber is cut using a high-quality fiber cleaver so that a precise cut and a flat end is found. Then, the fibers were cleaned with alcohol before being spliced. Finally, the multi-mode fiber (50/125 μm, NA = 0.20) of length 8.5 cm which has been optimized for better resolution is sandwiched between two step-index single-mode optical fibers (9/125 μm, NA = 0.14) using an electric type Fusion Splicer (Fujikura-60 s). The SMS fabricated here used mul-

Table 1
Optimization of slope length of SMS with length of MMF.

Length of MMF	Highest slope length in the SMS spectrum
8.2 cm	~6.8 nm
8.5 cm	~8.0 nm
8.7 cm	~6.66 nm
9.2 cm	~5.35 nm
9.4 cm	~6.0 nm

timode step-index fiber with core/cladding diameter of 50/125 μm and SMF with a core-cladding diameter of 8.2/125 μm.

We have optimised the MMF length for better resolution as shown in the Table1.

From the above table, it is clear that 8.5 cm length of the MMF could be used for the fabrication of SMS to achieve the high-resolution sensor. The higher slope lengths depend on the coupling condition of the modes between the SMS and MMF, Splicing condition and the MMF length.

From the Fig. 3 (a), it is observed that the slope regions are appearing similar for different trials. Hence, higher repeatability of the proposed SMS structure can be achieved. Furthermore, with an increase in the length of MMF section, the corresponding spectral location (as an edge filter) shifts to a shorter wavelength as can be seen from Fig. 3 (b), which is supported by (Application, 2006). Therefore, according to the application requirements (the desired wavelength region), an optimal spectral response can be achieved optimal choosing the length of the MMF section.

4. Analysis of the FBG sensor using interrogation method

In this section, the performance of this interrogation has been verified by theoretical and experimental analysis of the temperature and strain measuring FBG sensor. Besides, an enhancement of the proposed scheme has been investigated and compared further with the methods of using OSA.

4.1. Temperature and strain sensing

4.1.1. Theoretical analysis

In this part, we have analysed theoretically, the change in the reflected power from the unetched-FBG due to the external perturbation i.e., temperature and strain using OTDR.

The optical power reflected from an FBG is determined by the overlap integral of Power Spectral Density (PSD) of the Probe Pulse $S_{LS}(\lambda)$ and the FBG spectral reflectance $r(\lambda, \lambda_{BR})$ (Vasiljev et al., 2005; Kulchin et al., 2007):

$$P_R(\lambda_{BR}) = \int_0^{\alpha} S_{LS}(\lambda) r(\lambda, \lambda_{BR}) d\lambda \tag{5}$$

where λ_{BR} is the FBG resonance wavelength. Based on the reported results, we assume that the wavelength dependence of the spectral reflectance of the FBG is described with a Gaussian function whose half-width is represented as:

$$\Lambda_{FBG} \cong \lambda_{BR} \sqrt{\left(\frac{0.4\Delta n_{\ mod}}{n_{eff}}\right)^2 + \left(\frac{\Lambda_{\ mod}}{L}\right)^2} \tag{6}$$

where, L, $\Lambda_{\ mod}$,$\Delta n_{\ mod}$ and n_{eff} are the Length of the FBG, Modulation Period of RI, the Modulation depth of the RI and effective refractive index respectively.

Assuming that OTDR works in the multimode regime, so the power spectrum can be represented as:

$$S_{LS}(\lambda) \approx A(\lambda) F(\lambda) \tag{7}$$

where, $A(\lambda) = A_0 \exp\left(-\left(\frac{\lambda - \lambda_S}{\Delta\lambda_S}\right)^2\right)$ and $F(\lambda) = \exp\left(-\left(\frac{\lambda - i\lambda_0}{\Delta\lambda_0}\right)^2\right)$

are the functions that describe the PSD envelope and peaks of the probe pulse respectively. A_0 is the maximum PSD of the probe pulse and λ_S, $\Delta\lambda_S$, λ_0 are parameters determined by the property of the cavity of the light source.

Expanding (5) in Taylor series accurate to the first term and assume that $\Lambda_{FBG} \ll \Delta\lambda_S$, the variations in the reflected radiation power with a variation in the FBG wavelength (due to temperature and strain) can be calculated as:

$$\Delta P = \left(\frac{d}{d\lambda} A(\lambda_{BR})\right) \Lambda_{FBG} \Delta\lambda_{FBG} \tag{8}$$

where, $\Delta\lambda_{FBG} = 2n_{eff}\Lambda_{\ mod}\ (\alpha_1 \varepsilon + \alpha_2 \Delta T)$; α_1 and α_2 are the coefficients determined from the fiber material.

From the above equation (8), it can be seen that the change in the radiation power reflected from FBG with the variation in strain and temperature can be determined theoretically. The losses due to the connectors and splicing are neglected in the above consideration.

4.1.2. Performance analysis of the proposed sensor

The temperature and strain sensitivity of the proposed sensor can be determined using the interrogation technique where the FBG's spectral variations are straightforwardly translated into optical power variations.

In order to determine the temperature and strain coefficients, temperature and strain changes were applied to the grating separately. Our experimental and simulated results shown in Fig. 4 (a).

By changing the temperature between 20 °C to 200 °C with a step of 5 °C under a constant strain, we have measured the power variations of reflected light from FBG peak utilizing OTDR. Fig. 4 (a) shows the change of power of the FBG peak with increasing temperature, where a blue shift (i.e., negative slope) is observed due to the motive of using the edge filtering technique. With the increment of 5 °C, we main-

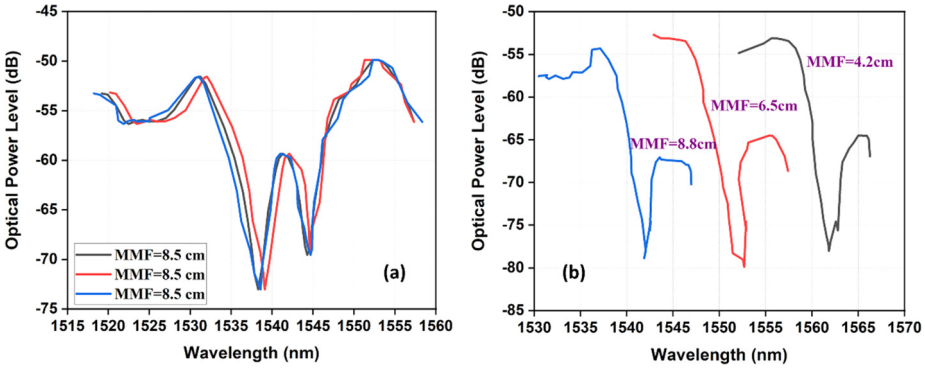

Fig. 3. (a) Different transmission spectra of SMS for the length of MMF = 8.5 cm and (b) SMS Spectra for different lengths of MMF. Only the filtering portion i.e., the falling edge region has taken into consideration.

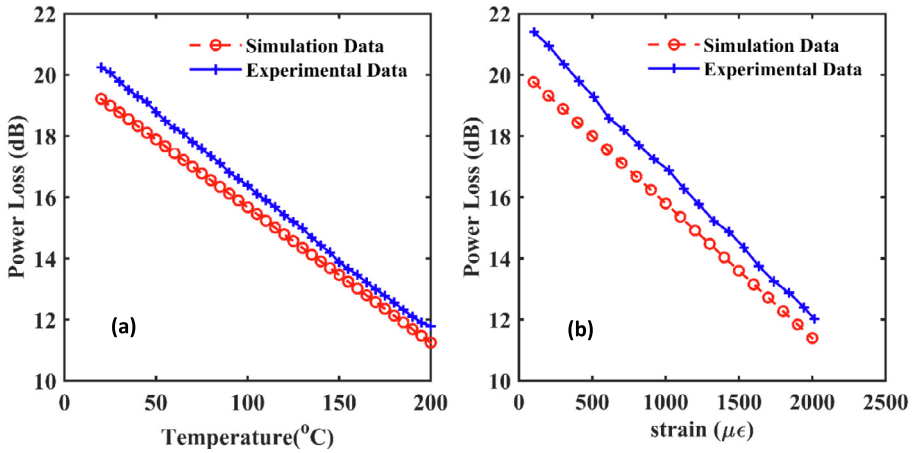

Fig. 4. Theoretical and experimental verification of (a) Power loss vs. change in temperature on unetched-FBG and (b) Power loss vs. applied strain on FBG. Parameters used for simulation are $\Lambda_{FBG} = 0.30nm$, $\Lambda_{mod} = 0.51\mu m$, $\lambda_{BR} = 1533nm$, $L = 1cm$, $\Delta n_{mod} = 7.5 \times 10^{-5}$, $\alpha_1 = 0.78$ and $\alpha_2 = 6.4 \times 10^{-6}$.

tained the temperature for 5 min to avoid and/or minimize any temperature fluctuation errors.

To evaluate the strain sensitivity, the experiments were carried out by increasing the strain from 100 με to 2015 με with a step of 103 με at room temperature (25 °C) with the tolerance of ±1 °C. A vibration-free table is used and sufficient time is allowed to avoid loading transients. It can be observed from the behaviour of the power as shown in Fig. 4 (b), that the behaviour of the power as strain on FBG increases, the optical intensity of the FBG decreases. It also, shows that the theoretical and experimental data are very close to each other.

The temperature and strain are monitored between the ranges of 20 °C to 200 °C and 100 με to 2015 με respectively which are limited due to the limitation of the oven and cantilever set-up used for characterization and by the quality of the FBG. We observed a higher loss when the experiment is carried out, due to the several physical phenomena such as splicing, insertion, and bending losses and surrounding environmental interferences of the SMS.

From the figures below we can estimate the temperature and strain sensitivities are about 1.01×10^{-2} dB/°C ($R^2 = 0.9984$) and 3.9×10^{-4} dB/με ($R^2 = 0.9981$) respectively.

4.2. Analysis of etched FBG with enhanced sensitivity

Hence, an analysis of enhancing the sensitivity using chemically-etched FBG is performed with the proposed interrogation technique. The etched FBG with a diameter of around 12 μm has been deployed in lieu of an un-etched FBG. It has been optimized such that cladding with reduced diameter can sustain the aforementioned range of strain and also to ensure that the propagating modes are affected by the surrounding medium.

When we etched the FBG to remove the cladding part adequately from the fiber, we pave the way to strengthen the "Evanescent field wave (EFW)". Once EFW strengthens, the sensitivity of the device increases (Sridevi et al., 2016; Korganbayev et al., 2018; Dey et al., 2020).

For this purpose, the FBG was etched chemically using Hydrofluoric acid in an optimized way and the effectiveness of the etching technique is monitored analysing the optical images captured by an inverted microscope (AE2000, Motic). Fig. 4 shows the microscopic images, where Fig. 5 (a) depicts the unetched FBG fiber while Fig. 5 (b) shows the etched fiber of diameter 12 μm. Images acquired at different places along the length of the fiber were essentially identical, demonstrating that etching was uniform throughout the length.

4.2.1. Experimental measurements

Here, the experimental results for enhancing the sensitivity of the proposed interrogation scheme are presented through temperature and strain measurements with up to 200 °C and 2015 με strain applied to the sensor, as shown in the Fig. 6 (a) and (b) respectively.

A remarkable change in the reflected power collected by OTDR has observed during the measurement of the aforementioned parameters compare to the changes observed in the case of un-etched FBG (see Fig. 4).

As the temperature and strain increase, power decreases linearly in both cases. The higher power loss is observed due to the employing of etched FBG where the cladding part was removed adequately to strengthen the EFW. Good linear behaviour is observed with high quality of linear fit (>0.99) as shown in Fig. 6. The temperature and strain sensitivities of the Bragg gratings are measured to be 6.7×10^{-2} dB/°C and 3.2×10^{-3} dB/με, respectively. Besides, the mean deviation of the temperature sensing is about 3.48%, while that of the strain sensing is about 4.03%. These deviation coefficients could be caused due to the existence of the environmental change which causes the instability of the SMS spectrum, inaccuracy in the cantilever set-up, fiber sliding effect, spectral flatness and noise-induced by the source. These could be minimized by designing a better SMS housing, modifying the applied loading set-up and a light source with high spectral flatness.

An enhancement of the sensitivity was observed due to decrease in Young's modulus of the etched fiber which increases its thermal expansion co-efficient and having a considerable influence on the thermal sensitivity of the sensor and the EFW which leads to the decrease of the thermo-optic coefficient of the fiber.

The OTDR system itself has an intrinsic measuring accuracy of 0.05 dB. Therefore, it has about 0.75 °C resolution in temperature and 15 με accuracies for strain measurement. Further, 0.01 nm random variation of the central wavelength of the FBG will induce intensity uncertainty of about 0.008 dB.

4.2.2. Comparing the performance of the proposed technique with OSA

To compare the performance of the proposed interrogation method in terms of sensitivity with the popular and standard reported meth-

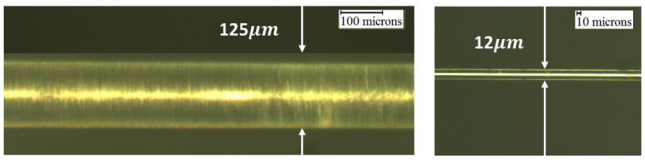

Fig. 5. Microscopic image of etched FBG. (a)unetched part of the grating (125 μm), scale bar 100 μm and (b) etched part of the grating (12 μm), scale bar 10 μm.

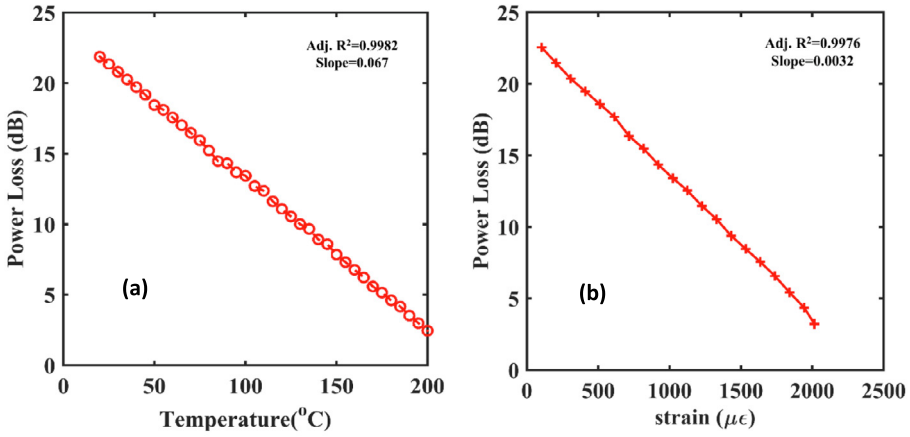

Fig. 6. (a) Power loss vs. temperature and (b) power loss vs. strain for the etched FBG using OTDR.

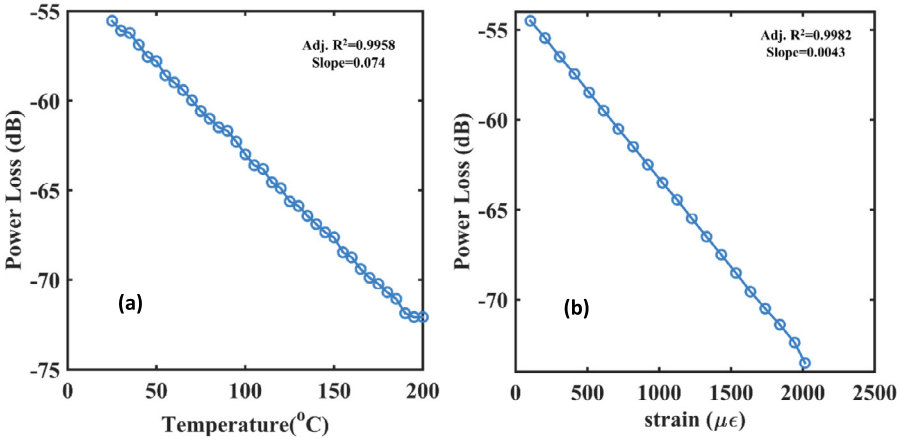

Fig. 7. (a) Power loss vs. temperature and (b) power loss vs. strain for the etched FBG using OSA.

Table 2
Comparison of relevant parameters of several schemes and the proposed approach highlighted in bold.

Items	Measurement Range (Temp & Strain)	Sensitivity (Temp & Strain)		Resolution
		Value	Remarks	
WTFCL + TLS + EDFA + SOA + FBG (Wang et al., 2015)	NA	NA	–	NA
	0-1200 με	7.60 × 10^{-3}dB/με	Moderate	
FBG + LPG + OTDR (Hatta et al., 2013)	20–60 °C	5.90 × 10^{-3} dB/°C	Moderate	0.17 °C
	0–500 με	4.20 × 10^{-4} dB/με	Moderate	2.32 με
FBG + OTDR (Zhang et al., 2003)	30–200 °C	1.7 × 10^{-3} dB/°C	Moderate	1 °C
	0–1800 με	3.65 × 10^{-3}dB/με	Moderate	–
This Work (FBG + SMS + OTDR)	20–200 °C	6.7×10^{-2}dB/°C	High	0.75 °C
	100–2015 με	3.20×10^{-3}dB/με	Moderate	15 με

*NA = Not Available.

ods, we have employed the OSA (Agilent 86142B) instead of the OTDR in the sensing circuitry to track the change of the FBG peak with the change of the temperature and strain.

For measuring the temperature and strain sensitivity, when the temperature and strain were applied on the grating, the wavelength shift produces a change in the output.

Fig. 7 (a) and (b) show a typical relationship between the power loss of the FBG peak with the temperature and strain applied on the FBG, respectively. The achieved sensitivities are 7.4 × 10^{-2} dB/°C and 4.3 × 10^{-3} dB/με for temperature and strain, respectively of the proposed sensor using OSA. These obtained sensitivities are almost near to the sensitivities obtained using OTDR. As the OSA has the inherent measurement accuracy in the power of 0.14 dB, then the resolution in temperature is about 1.8 °C while for strain measurement is about 32 με. In fact, for measuring the reflected power, the resolution of OTDR is better than OSA.

Hence, this OTDR can be used instead of OSA where the analysis of power reflected from the grating, the budget and the resolution are of the paramount importance in the field of sensing applications.

A comparative study is presented in Table 2 as shown below. Here the performance of our proposed sensor is tallied against few reported results for measuring temperature and strain using different interrogation-based methods.

Analysing the following table, it is clear that our proposed technique is well-positioned among different methods found in the past literature, yields high sensitivity with higher measurement range and cost-effectiveness over the other reported methods.

5. Conclusions

In conclusion, a simple, fast, easy to operate and economical OTDR based interrogation technique exploring edge filtering property of optimized SMS has been presented here. To our best knowledge, such SMS, OTDR interrogation technique by convolute ing FBG for measuring temperature and strain sensor is not reported yet. The experimental analysis has also been verified theoretically with the close agreement.

In the experimental analysis, the temperature and strain sensitivity using the proposed interrogation method using un-etched FBG was measured to be 10.1×10^{-3} dB/℃ and 3.9×10^{-4} dB/με, respectively. The method was also demonstrated with etched FBG for enhancing the sensitivity. Using the etched FBG, enhanced sensitivity of 6.7×10^{-2} dB/℃ and 3.2×10^{-3} dB/με were recorded with a higher resolution of ±0.75 ℃ and ±15 με for temperature and strain, respectively. The obtained results were compared with OSA. A better resolution can be obtained using a high-quality ODTR with higher accuracy. Hence, OTDR can be used as an alternate of OSA in the interrogation or multiplexing system. The performance of our proposed sensor has been tailed against the reported methods for measuring temperature and strain, where the proposed sensor is well-positioned. As OTDR is a cost-effective, handy and widely available instrument in the market, so this proposed method is cost-effective and has obtained good results in comparison to earlier reports. Since the intensity is being measured, the dynamic response also expected to be better. Our sensor configuration offers numerous advantages over earlier reported methods, including high intrinsic sensitivity, easy fabrication technique and it is economical. To resolve the input power fluctuation, the output power difference can be normalized with the input power. The Edge filter SMS with proper encapsulation can be kept in a temperature stabilized region. Hence, there will be less chance of getting temperature induced interrogation error.

To take the maximum advantages of the method, the optimum parameters such as slope rage of the steep edge in the SMS spectrum, peak reflectivity of the FBG at the central wavelength, the diameter of the cladding can be investigated for further studies. Exploring the feature of spatial tracing of OTDR, multiple FBGs can be deployed to design a quasi-distributed sensor. The designed sensor may find applications for simultaneous strain and temperature measurement in structural health monitoring, spatial analysis of engineering structures and fusion reactor relevant applications.

Declaration of Competing Interest

The authors declare that they have no known competing financial interests or personal relationships that could have appeared to influence the work reported in this paper.

Acknowledgements

The authors are thankful to BRNS (DAE), Government of India for the support by their funding (39/14/27/2016-BRNS/39064). Authors are also grateful to Dr C Hari Krishna for his valuable suggestions and fruitful discussions.

References

Loyez, M., Hassan, E.M., Lobry, M., Liu, F., Caucheteur, C., Wattiez, R., DeRosa, M.C., Willmore, W.G., Albert, J., 2015. Rapid detection of circulating breast cancer cells using a multiresonant optical fiber aptasensor with plasmonic amplification. ACS Sensors 5, 454–463.

Kinet, D., Megret, P., Goossen, K.W., Qiu, L., Heider, D., Caucheture, C., 2014. Fiber Bragg grating sensors toward structural health monitoring in composite materials: challenges and solutions. Sensors 14, 7394–7419.

Guerra, G., Lonardi, M., Galtarossa, A., Rusch, L.A., Bononi, A., Palmieri, L., 2019. Analysis of modal coupling due to birefringence and ellipticity in strongly guiding ring-core OAM fibers. Opt. Express 27, 8308–8326.

Berruti, G.M., Petagna, P., Buontempo, S., Makovec, A., Szillasi, Z., Beni, N., Consales, M., Cusano, A., 2016. One year of FBG-based thermo-hygrometers in operation in the CMS experiment at CERN. J Instrum 11, PO3007.

Leal-Junior, A., Theodosiou, A., Diaz, C., Marques, C., Pontes, M.J., Kalli, K., Frizera-neto, A., 2018. Polymer optical Fiber Bragg gratings in CYTOP Fibers for angle measurement with dynamic compensation. Polymers 10, 674.

Vaddadi, V.S.C.S., Parne, S.R., Afzulpurkar, S., Desai, S.P., Parambi, V.V., 2020. Design and development of pressure sensor based on Fiber Bragg Grating (FBG) for ocean applications. Eur. Phys. J. Appl. Phys. 90, 30501.

Chaudhuri, P.R., Pradhan, S., 2018. Demonstration of gain multiplication by series assembly of fiberoptic cantilever beam deflection: measurement of low magnetic field and magnetization of probe samples. Optik 172, 412–423.

Ma, Z., Chen, X., 2019. Fiber Bragg gratings sensors for aircraft wing shape measurement: recent applications and technical analysis. Sensors 19, 55.

Frazao, O., Marques, L.M., Baptista, J.M., 2006. Fiber Bragg grating interrogation based on high-birefringence Fiber loop mirror for strain-temperature discrimination. Microwave Opt. Technol. Lett. 48, 2326–2328.

Li, L., Tong, X.L., Zhou, C.M., Wen, H.Q., Lv, D.J., Ling, K., Wen, C.S., 2011. Interrogation of miniature Fabry-Perot Fiber optic sensor with FBG for the measurement of temperature and strain. Opt. Commun. 284, 1612–1615.

Diaz, C.A.R., Marques, C.A.F., Domingues, M.F.M., Riberio, M.R.N., Neto, A.F., Pontes, M.J., Andre, P.S., Antunes, P.F.C., 2018. A cost-effective edge-filter based FBG interrogator using catastrophic fuse effect micro-cavity interferometers. Measurement 124, 486–493.

Zhang, Po, Cerecedo-Nunez, H.H., Pickrell, B. Qi G., Wang, Anbo, 2003. Optical time-domain reflectometry interrogation of multiplexing low-reflectance Bragggrating-based sensor system. Opt. Eng. 42.

Nguyen, L.V., Hwang, D., Moon, D.S., Chung, Y., 2009. Simultaneous measurement of temperature and strain using a Lyot Fiber filter incorporated with a Fiber Bragg grating in a linear configuration. Meas. Sci. Technol. 20, 034006-1-5.

Uchimura, R., Wada, A., Tekuramori, S., Takeuchi, M., Tukida, O., Tanaka, S., Takahasi, N., 2014. Simultaneous measurement of temperature and static strain using FBG Fabry-Perot interferometer in polarization-maintaining Fiber. Proc. SPIE. 9157.

Xiong, L., Zhang, D., Li, L., Guo, Y., 2014. EFPI-FBG hybrid sensor for simultaneous measurement of high temperature and strain. Chin. Opt. Lett. 12, 120605-1-5.

Pan, Y., Liu, T., Jiang, J., Liu, K., Wang, S., Yin, J., He, P., Yan, J. Simultaneous Measurement of Temperature and Strain using Spheroidal-cavity-Overlapped FBG, IEEE Photonics J., 7, 6803406-1-6, (2015).

Liu, Q., Ran, Z.L., Rao, Y.J., Shu-cheng, L., Hui-Qin, Y., Ya, H., 2014. Highly integrated FP/FBG sensor for simultaneous measurement of high temperature and strain. IEEE Photon. Tech. Lett. 26, 1715–1717.

Markowski, K., Jedrzejewski, K., Marzecki, M., Osuch, T., 2017. Linearly chirped tapered Fiber-Bragg-grating-based Fabry-Perot cavity and its application in simultaneous strain and temperature measurement. Opt. Lett. 42, 1464–1467.

Ranjan, R., Esposito, F., Campopiano, S., Iadicicco, A., 2017. Sensing characteristics of Arc-induced Long period gratings in polarization-maintaining panda Fiber. IEEE Sens. J. 17, 6953–6959.

Ascorbe, J., Coelho, L., Santos, J.L., Frazao, O., Corres, J.M., 2018. Temperature compensated strain sensor based on long-period gratings and microspheres. IEEE Photon. Tech. Lett. 30, 67–70.

Esposito, F., Srivastava, A., Campopiano, S., Iadicicco, A., 2019. Multi-parameter sensor based on single Long Period Grating in Panda Fiber for the simultaneous measurement of SRI, temperature and strain. Opt Laser Technol. 113, 198–203.

Patrick, H., Williams, G.M., Kersey, A.D., Pedrazzani, J.R., Vengsarkar, A.M., 1996. Hybrid Fiber Bragg grating/long period grating sensor for strain/temperature discrimination. IEEE Photon. Tech. Lett. 8, 1223–1225.

Wu, Q., Hatta, A.M., Semenova, Y., Farrell, G., 2009. Use of a single-multiple-single-mode Fiber filter for interrogating Fiber Bragg grating strain sensors with dynamic temperature compensation. Appl. Opt. 48, 5451–5458.

Barrera, D., Sales, S., 2013. A High-Temperature Fiber Sensor Using a Low-Cost Interrogation Scheme. Sensors 13, 11653–11659.

Wang, P., Ding, M., Bo, L., Guan, C., Semenova, Y., Wu, Q., Farrell, G., Brambilla, G., 2013. Fiber-tip high-temperature sensor based on multimode interference. Opt. Lett. 38, 4617–4620.

Tian, K., Farrell, G., Wang, X., Yang, W., Xin, Y., Liang, H., Lewis, E., Wang, P., 2017. Strain sensor based on gourd-shaped single-mode multimode-single-mode hybrid optical fibre structure. Opt. Express 25, 18885–18896.

S. Stopiński, K. Anders, S. Szostak, and R. Piramidowicz, "Optical Time Domain Reflectometer Based on Application Specific Photonic Integrated Circuit," in 2019 Conference on Lasers and Electro-Optics Europe and European Quantum Electronics Conference, OSA Technical Digest (Optical Society of America, 2019), paper ch_p_38.

Yu-Lung, L., Shao-Hung, X. New sensing mechanism using an optical time domain reflectometry with fiber Bragg gratings, Sensor Actuat A-Phys, 136, 238-243, (2007).
Valente, L.C.G., Braga, A.M.B., Ribeiro, A.S., Regazzi, R.D., Ecke, W., Chojetzki, C., Willsch, R., 2002. Time and wavelength multiplexing of fiber bragg grating sensors using a commercial OTDR, OFS. IEEE 151–154.
Bravo, M., Fernandez, M., Lopez-Amo, M., 2012. Hybrid OTDR-fiber laser system for remote sensor multiplexing. IEEE Sens. J. 12, 174–177.
Bolognini, G., Park, J., Soto, A.M., Park, N., Pasquale, F. Di., 2007. Analysis of distributed temperature sensing based on Raman scattering using OTDR coding and discrete Raman amplification. Meas. Sci. Technol. 18, 3211–3218.
Zhang, P., Cerecedo-Nunez, H.H., Qi, B., Pickrell, G.R., Wang, A., 2003. Optical time domain reflectometry interrogation of multiplexing low-reflectance Bragg Grating-based sensor system. Opt. Eng. 42, 1597–1603.
Bravo, M., Lopez-Amo, M., Frazao, O., Bapista, J.M., Santos, J.L. New interrogation technique for multiplexing LPG-Fiber loop mirrors-based displacement sensors using an OTDR, IEEE Sens. Proc. (2011).
Hatta, A.M., Indriawati, K., Bestariyan, T., Humada, T., Sekartedjo, 2013. SMS Fiber structure for Temperature measurement using an OTDR. Photonics Sens. 3, 262–266.
Hatta, A.M., Permana, H.E., Setlejono, H., Kusumawardhani, A., Sekartedjo, 2013. Strain measurement based on SMS Fiber structure sensor and OTDR. Microw Opt. Techn. Let. 55, 2576–2578.
Wang, X., Yan, Z., Wang, F., Hua, J., Mou, C., Sun, Z., Zhang, X., Zhang, L., 2015. An OTDR and gratings assisted multifunctional fiber sensing system. IEEE Sens. J. 15, 4660–4666.
Song, Y., Xia, L., Wu, Y., 2019. The interrogation of quasi-distributed optical FBG sensing system through adopting a wavelength-tunable fiber chaotic laser. J. Lightw. Technol. 37, 2435–2442.
Kumar, A., Varshney, R.K., Siny, A.C., Sharma, P., 2003. Transmission characteristics of SMS Fiber optic sensor structures. Opt. Commun. 219, 215–219.
Hill, K.O., Meltz, G., 1997. Fiber Bragg grating technology fundamentals and overview. J. Lightw. Technol. 15, 1263–1276.
Multimode-Fiber-Based Edge Filter For Optical Wavelength Measurement Application and Its Design" Qian Wang and Gerald Farrell, Microw. Opt. Technol. Lett., (2006).
Vasiljev, S.A., Medvedkov, O.I., Korolov, I.G., Bozhkov, A.S., Kurkov, A.S., Dianov, E.N., 2005. Fiber gratings and their applications. Quantum Electron. 35, 1085–1103.
Kulchin, Yu.N., Vitrik, O.B., Shalagin, A., Mbabin, S.A., Vlasov, A.A., 2007. Application of optical time-domain reflectometry for the interrogation of fiber Bragg sensors. Laser Phys. 17, 1335–1339.
Sridevi, S., Vasu, K.S., Asokan, S., Sood, A.K., 2016. Enhanced strain and temperature sensing by reduced graphene oxide coated etched Fiber Bragg gratings. Opt. Lett. 41, 2604–2607.
Korganbayev, S., Ayupova, T., Sypabekova, M., Bekmurzayeva, A., Shaimerdenova, M., Dukenbayev, K., Molardi, C., Tosi, D., 2018. Partially etched chirped Fiber Bragg grating (pECFBG) for joint temperature, thermal profile, and refractive index detection. Opt. Exp. 26, 18708–18720.
Dey, K., Roy, S., Pavan, V.D.R., Sai, S.M., Ramesh, B., 2020. Interrogation of SMS for measuring strain and temperature using etched FBG with enhanced sensitivity. Proc. of SPIE 11355, 113550Z1-6.